Semiconducting charge-transfer salts of BEDT-TTF [bis(ethylenedithio)tetrathiafulvalene] with hexachlorometallate(IV) anions

Cameron J. Kepert,† Mohamedally Kurmoo‡ and Peter Day*

Davy Faraday Research Laboratory, The Royal Institution, 21 Albemarle Street, London, UK W1X 4BS

Two new crystalline charge-transfer salts of BEDT-TTF [bis(ethylenedithio)tetrathiafulvalene] containing hexachlorometallate anions of 5d elements have been synthesised, characterised structurally and their magnetic and conducting behaviour investigated. α-(BEDT-TTF)$_4$[ReCl$_6$]·C$_6$H$_5$CN is triclinic [$P\bar{1}$; $a=9.455(2)$, $b=11.306(3)$, $c=18.193(5)$ Å; $\alpha=101.85(2)$, $\beta=92.74(2)$, $\gamma=110.52(2)^\circ$; $Z=1$]. Its structure consists of alternate layers of BEDT-TTF and of [ReCl$_6$]$^{2-}$·C$_6$H$_5$CN, the former consisting of two crystallographically independent stacks, in one of which the molecules carry a charge close to +1 while in the other they are approximately neutral. The cations lie between the [ReCl$_6$]$^{2-}$ moieties while the neutral molecules are closest to the C$_6$H$_5$CN species showing that the structure is determined by electrostatic interactions. (BEDT-TTF)$_2$[IrCl$_6$] is likewise triclinic [$P\bar{1}$; $a=8.721(1)$, $b=10.257(2)$, $c=11.086(2)$ Å; $\alpha=111.00(1)$, $\beta=98.31(1)$, $\gamma=103.32(1)^\circ$; $Z=1$]. Its packing motif is new among BEDT-TTF salts, containing no discrete layers of anions and cations. Face-to-face BEDT-TTF dimers form an infinite three-dimensional network. Both compounds are semiconducting and their magnetic properties are dominated by the Curie–Weiss behaviour of the anions.

Although they give rise to a large number of superconducting phases with the TMTSF (tetramethyltetraselenafulvalene) donor molecule, octahedral anions have received relatively little attention among the charge-transfer salts of BEDT-TTF. The only BEDT-TTF salts with dinegative octahedral anions are the κ-(BEDT-TTF)$_4$[MX$_6$]·C$_6$H$_5$CN series ([MX$_6$]$^{2-}$ = [PtCl$_6$]$^{2-}$, [PtBr$_6$]$^{2-}$, [TeCl$_6$]$^{2-}$, [SnCl$_6$]$^{2-}$).[1] The [PtCl$_6$]$^{2-}$ salt is unique among these in having semi-metallic properties, although it undergoes a first-order metal–insulator transition near 250 K. It differs structurally from the other members by a doubling of the unit cell at high temperature,[2] and appears to be the only salt of BEDT-TTF with two independent BEDT-TTF layers showing semi-metallic and semiconducting properties. It is of interest to attempt to stabilise the metallic κ-phase layer to low temperature by substituting different octahedral anions. To combine the possibility of including magnetic moments and anions with redox possibilities we have synthesised new BEDT-TTF salts of [ReCl$_6$]$^{2-}$ and [IrCl$_6$]$^{2-}$. Low-spin 5d^5 [IrCl$_6$]$^{2-}$ is a strong oxidising agent, converting to the diamagnetic d^6 [IrCl$_6$]$^{3-}$ anion, and 5d^3 [ReCl$_6$]$^{2-}$ has previously been reported to form a semiconducting salt with dibenzotetrathiafulvalene.[3] This paper presents the synthesis, crystal structure and physical properties characterisation of α-(BEDT-TTF)$_4$[ReCl$_6$]·C$_6$H$_5$CN and (BEDT-TTF)$_2$[IrCl$_6$].

Experimental

Syntheses

(NBu$^n_4$)$_2$[ReCl$_6$] was prepared by metathesis. Solutions of K$_2$[ReCl$_6$] (0.96 g, Aldrich) and NBu$^n_4$Cl·xH$_2$O (1.52 g, excess) in dilute hydrochloric acid were added and evaporated to small volume. Recrystallisation from dichloromethane and diethyl ether produced long green–yellow needles.

Concentrated aqueous solutions of H$_2$[IrCl$_6$]·xH$_2$O (0.21 g, Aldrich) and NEt$_4$Cl (0.23 g) were mixed and evaporated to a small volume and the dark brown precipitate was collected and recrystallised from dilute hydrochloric acid to form small block-like crystals of (NEt$_4$)$_2$[IrCl$_6$].

Electrochemical synthesis

Crystals were grown electrochemically on Pt electrodes in conventional H-shaped cells (45 cm^3 capacity). Approximately 20 mg of BEDT-TTF, twice recrystallised from CHCl$_3$, was added to the anodic section of the cell, and a solution of the anion salt (*ca.* 20 mg) was added to all three compartments. The cells were set up under an atmosphere of dry Ar and placed in a dark enclosure on a vibration free table. With (NBu$^n_4$)$_2$[ReCl$_6$] as electrolyte, benzonitrile as solvent and a current of 0.5 μA, high-quality, thick, black, hexagonal plates (*ca.* $2\times2\times0.2$ mm^3) of α-(BEDT-TTF)$_4$[ReCl$_6$]·C$_6$H$_5$CN formed on the anode.

With (NBu$^n_4$)$_2$[IrCl$_6$] as electrolyte and dichloromethane as solvent, low-quality, black, polycrystalline material coated the anodes on passing a current of 0.3–0.5 μA. On the other hand, in benzonitrile with a current of 0.5 μA (voltage *ca.* 2.6 V), high-quality, black, block-like crystals ($1\times1\times1$ mm^3) of (BEDT-TTF)$_2$[IrCl$_6$] formed on the anode. Most of these were kite-shaped, owing to the presence of a clearly visible diagonal twin plane.

Crystal structure determination

α-(BEDT-TTF)$_4$[ReCl$_6$]·C$_6$H$_5$CN. The unit cell was refined from 25 reflections ($22.9<2\theta<30.6^\circ$). The hydrogen atoms of the BEDT-TTF ethylene groups were fixed with regular geometry at a distance of 0.96 Å from the carbon atoms. PSI-scan data were collected on ten reflections. In the least-squares structural refinement the analytical absorption correction was superior to the laminar empirical correction, giving a lower R-factor of refinement [for reflections from the full data set with $I\geqslant3\sigma(I)$, $R=5.39\%$ *cf.* 5.56%] and preventing the omission of 745 reflections. The reflections (2,0,1), (2,$\bar{2}$,1), (2,$\bar{3}$,1), (2,$\bar{3}$,2) and (2,1,1) were found to suffer significantly from extinction (each with $-\mathrm{dev}/\sigma>8$), and were omitted from the least-squares refinement. Despite the general bad agreement of the intense reflections, the application and refinement of the

† Present address: Inorganic Chemistry Laboratory, South Parks Road, Oxford, UK OX1 3QY.
‡ Present address: IPCMS-GMI, 23 rue Loess, BP 20/CR, 67037 Strasbourg Cedex, France.

weighting scheme

$$w(S)=\frac{1}{\sigma^2(S)+g|F_{obs}(S)|^2}$$

where $\sigma(S)$ is the estimated standard deviation of $F(S)$, and g must be positive, led to a significant increase in the R-factors and only a small decrease in the e.s.d.s. The weighting parameter g was subsequently set to zero. Further details of the data collection, processing and structural refinement may be found in Table 1.

(BEDT-TTF)$_2$[IrCl$_6$]. A region was cut from a large diagonally twinned crystal, and confirmed to be single-phase by X-ray oscillation photography. The unit cell was refined from 25 reflections ($17.6<2\theta<26.8^\circ$). PSI-scan data were collected on ten reflections. The data were corrected for absorption by the empirical ellipsoid method. No significant change was seen in the refinement indices, apart from a slight lowering of the goodness of fit. All BEDT-TTF ethylene group hydrogen atoms were located in the Fourier difference map. The positional and isotropic thermal parameters for H(10B) were unstable to refinement and hence were fixed, whilst all others refined to give reasonable values. Further details of the data collection, processing and structural refinement may be found in Table 1.

Electrical conductivity

The electrical conductivities of single crystals of both salts were determined, for the $ReCl_6$ salt by both two- and four-probe dc methods parallel and perpendicular to the crystal plates from 300 to 85 K, and for the $IrCl_6$ salt by two-probe measurements from 300 to 180 K.

Magnetism

The magnetic susceptibilities of polycrystalline samples of both salts were determined from 300 to 2 K in fields of 250 and 1000 G ($ReCl_6$) and 5000 G ($IrCl_6$) using a Quantum Design MPMS 7 SQUID magnetometer. Samples were mounted inside a Perspex rod centred on the axis of the magnet solenoid. Magnetisation measurements were also made in fields from 0.1 to 7.0 T at 2 and 5 K. Corrections were made for the diamagnetic response of the sample rod and of the sample using Pascal's constants.

Electronic band structure

Band-structure calculations were performed in the tight binding formalism within the dimer-splitting approximation using the extended Hückel method, with a double-zeta basis set.[4]

Results and Discussion

Crystal and electronic band structures of α-(BEDT-TTF)$_4$[ReCl$_6$]·C$_6$H$_5$CN

The salt crystallises in the $P\bar{1}$ space group, and has a comparable unit cell to the low-temperature (single-layer) phase of κ-(BEDT-TTF)$_4$[PtCl$_6$]·C$_6$H$_5$CN {α-(BEDT-TTF)$_4$[ReCl$_6$]·C$_6$H$_5$CN: $a=9.455$, $b=11.306$, $c=18.193$ Å, $\alpha=101.85$, $\beta=92.74$, $\gamma=110.52^\circ$, $V=1767.3$ Å^3; κ-(BEDT-TTF)$_4$[PtCl$_6$]·C$_6$H$_5$CN at 218 K:[2] $a=8.582$, $b=11.891$, $c=17.512$ Å, $\alpha=81.55$, $\beta=86.65$, $\gamma=94.44^\circ$, $V=1758$ Å^3}. The asymmetric unit contains two BEDT-TTF molecules, one half of the [ReCl$_6$] unit, and a 50% occupied benzonitrile molecule [see Fig. 1(*a*) for the atomic numbering scheme]. Ionic layers of α-packed 2(BEDT-TTF$_2$)$^+$ and [ReCl$_6$]$^{2-}$·C$_6$H$_5$CN alternate along the

Table 1 Crystal and refinement data for α-(BEDT-TTF)$_4$[ReCl$_6$]·C$_6$H$_5$CN and (BEDT-TTF)$_2$[IrCl$_6$]

	α-(BEDT-TTF)$_4$[ReCl$_6$]·C$_6$H$_5$CN	(BEDT-TTF)$_2$[IrCl$_6$]
crystal data		
chemical formula	$C_{47}H_{37}Cl_6N_1Re_1S_{32}$	$C_{20}H_{16}Cl_6Ir_1S_{16}$
M/g mol^{-1}	2040.7	1174.2
crystal system	triclinic	triclinic
space group	$P\bar{1}$	$P\bar{1}$
a/Å	9.455(2)	8.721(1)
b/Å	11.306(3)	10.257(2)
c/Å	18.193(5)	11.086(2)
α/degrees	101.85(2)	111.00(1)
β/degrees	92.74(2)	98.31(1)
γ/degrees	110.52(2)	103.32(1)
V/Å^3	1767.3(8)	872.2(3)
Z	1	1
$F(000)$	1015	571
D_c/g cm^{-3}	1.92	2.25
crystal size/mm^3	0.10 × 0.40 × 0.50	0.15 × 0.15 × 0.30
μ(Mo-Kα)/cm^{-1}	29.2	52.2
data collection and processing		
data measured	8213	3290
unique data	6233	3078
sigma cut (c)	5	3
no. with $I \geqslant c\sigma(I)$	5298	2910
structural analysis and refinement		
no. parameters	390	225
absorption corr.	analytical	empirical
crystal faces (distance from crystal centre)	001 (0.05)	—
	010 (0.25)	—
	1$\bar{1}$0 (0.20)	—
μR	—	0.65
min., max. transmission	0.35, 0.75	0.42, 0.46
g (weighting)	0.00	0.00
R(%) [R(all) (%)]	4.97 (6.22)	3.27 (3.68)
R_w (%)	4.41	2.87
goodness of fit	3.70	1.81
largest peak/e Å^{-3}	1.2, −1.7	0.9, −0.5

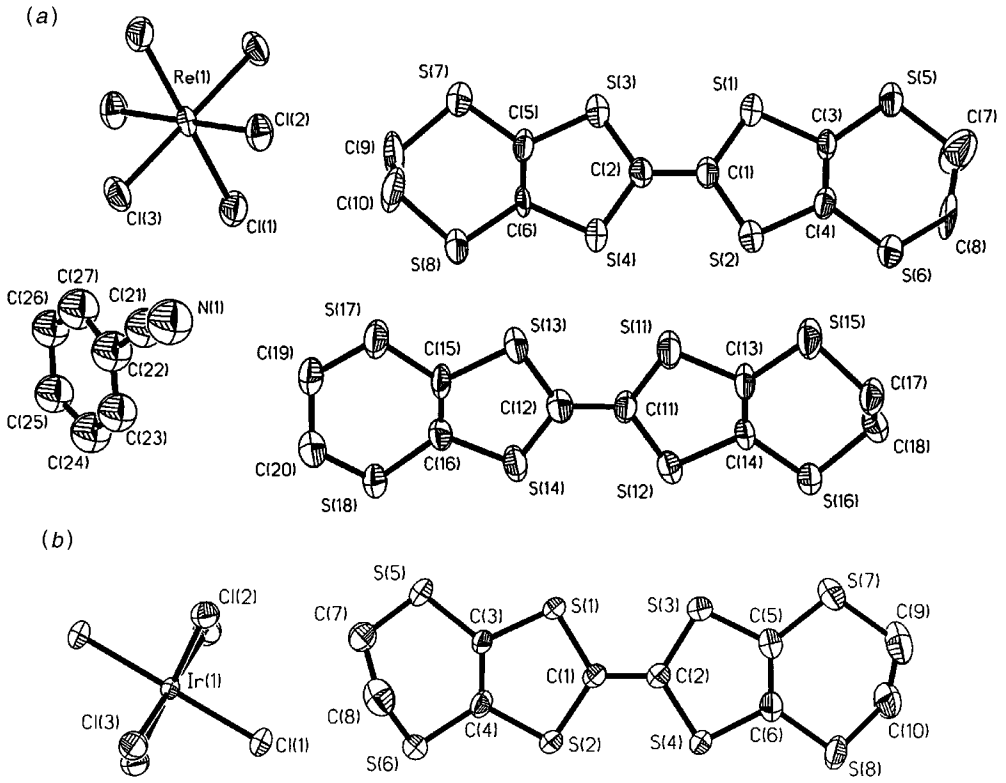

Fig. 1 Atomic numbering scheme of (*a*) α-(BEDT-TTF)$_4$[ReCl$_6$]·C$_6$H$_5$CN and (*b*) (BEDT-TTF)$_2$[IrCl$_6$] (both showing 50% thermal ellipsoids)

c-direction (see Fig. 2). Atomic coordinates, thermal parameters, and bond lengths and angles have been deposited at the Cambridge Crystallographic Data Centre (CCDC). See Information for Authors, *J. Mater. Chem.*, 1997, Issue 1. Any request to the CCDC for this material should quote the full literature citation and the reference number 1145/22. Selected intramolecular bond lengths and angles are listed in Table 2, and the shortest intermolecular S—S distances may be found adjacent to the calculated intermolecular transfer integrals in Table 3.

BEDT-TTF layer. The BEDT-TTF molecules form a layer in which the packing is of the α-type.[5] The layer is constructed of two crystallographically independent stacks of BEDT-TTF, with a dihedral angle of 120.0°. Inversion centres are positioned midway between each parallel BEDT-TTF pair, leading to AA* and BB* stacks that propagate along the *a*-direction. From Fig. 2 it can be seen that the two BEDT-TTF molecules lie at approximately the same height within the layer. The AA*A and BB*B pairs of stacking interactions are very similar, with alternating translations of 0 and 1/4 along the long axis of the molecule. The intermolecular spacings within each stack are unusually wide, with at most one intermolecular S—S distance less than 4 Å for each interaction (see Table 3). In contrast, there are numerous short interstack S—S distances. It seems likely that anion–anion repulsion causes the enhanced separation between the BEDT-TTF in this direction.

The long axes of molecules A and B make angles of 66.9° and 65.7° respectively with the plane of the BEDT-TTF layer, giving an effective perpendicular cross-sectional area per molecule of 22.9 Å^2, similar to many other close-packed BEDT-TTF salts. All four independent ethylene groups are ordered in the chair form and both molecules adopt the staggered conformation.

Analysis of the intramolecular bond lengths of the two independent BEDT-TTF molecules suggests that the two stacks have quite different degrees of ionicity, with calculated charges $Q(A)=0.8(2)+$ and $Q(B)=0.4(2)+$ as estimated by

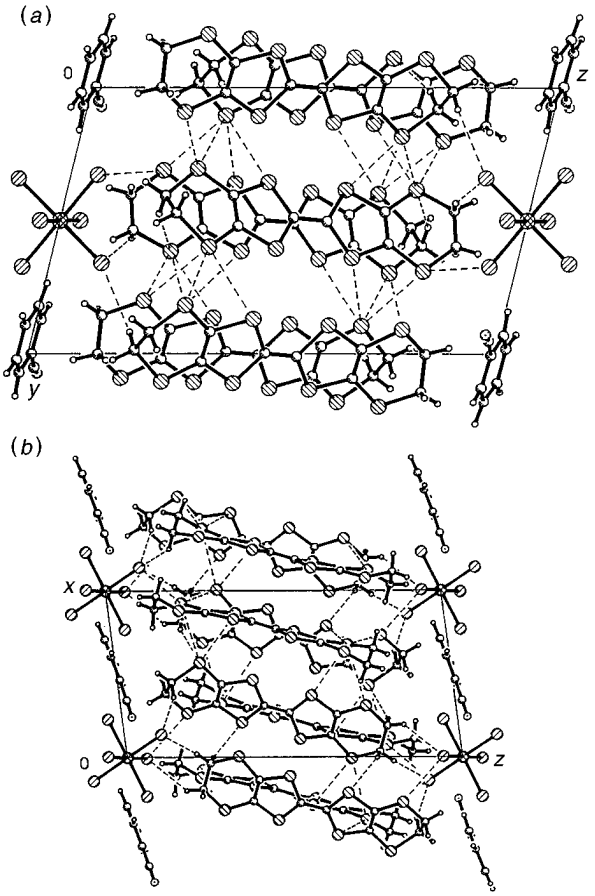

Fig. 2 Projection of α-(BEDT-TTF)$_4$[ReCl$_6$]·C$_6$H$_5$CN (*a*) down the *a* axis; (*b*) down the *b* axis (for clarity only one orientation of the disordered C$_6$H$_5$CN molecule is shown)

Table 2 Selected intramolecular bond lengths (Å) and angles (degrees) of α-(BEDT-TTF)$_4$[ReCl$_6$]·C$_6$H$_5$CN

Re(1)—Cl(1)	2.365(3)	N(1)—C(21)	1.01(5)
Re(1)—Cl(2)	2.371(3)	C(21)—C(22)	1.54(6)
Re(1)—Cl(3)	2.361(2)	C(22)—C(27)	1.46(4)
		C(23)—C(24)	1.37(5)
Cl(1)—Re(1)—Cl(2)	91.5(1)	C(24)—C(25)	1.36(4)
Cl(1)—Re(1)—Cl(3)	88.5(1)	C(25)—C(26)	1.46(5)
Cl(2)—Re(1)—Cl(3)	88.9(1)	C(26)—C(27)	1.23(5)
S(1)—C(1)	1.727(8)	S(11)—C(11)	1.731(13)
S(1)—C(3)	1.760(11)	S(11)—C(13)	1.776(12)
S(2)—C(1)	1.723(10)	S(12)—C(11)	1.746(13)
S(2)—C(4)	1.735(10)	S(12)—C(14)	1.759(11)
S(3)—C(2)	1.725(11)	S(13)—C(12)	1.748(13)
S(3)—C(5)	1.746(10)	S(13)—C(15)	1.760(11)
S(4)—C(2)	1.737(9)	S(14)—C(12)	1.737(13)
S(4)—C(6)	1.743(10)	S(14)—C(16)	1.765(12)
C(1)—C(2)	1.390(15)	C(11)—C(12)	1.376(15)
C(3)—C(4)	1.342(12)	C(13)—C(14)	1.322(18)
C(5)—C(6)	1.346(12)	C(15)—C(16)	1.327(18)

the δ-model.[6] The A stacks are sandwiched between chains of [ReCl$_6$]$^{2-}$ anions, whereas the B stacks lie between the neutral benzonitrile solvent molecules [Fig. 3(*a*)]. Thus electrostatic interaction with the anion layer may influence electronic localisation strongly within the BEDT-TTF layer, as in κ-(BEDT-TTF)$_4$[PtCl$_6$]·C$_6$H$_5$CN. Such an effect (not previously noted) is a pervasive contributor to localisation in BEDT-TTF salts in general.

Anion layer. The structure of the anion–solvent layer [Fig. 3(*b*)] is the same as that found in κ-(BEDT-TTF)$_4$[PtCl$_6$]·C$_6$H$_5$CN,[1] although modified slightly owing to changes to the *a*, *b* and γ unit-cell parameters (brought about by the different donor packing arrangement). The average Re—Cl bond length of 2.366 Å is slightly longer than the Pt—Cl length of 2.318 Å. The area of the *ab* plane is 100.1 Å^2, in comparison to the similar value of 103.2 Å^2 for κ-(BEDT-TTF)$_4$[PtCl$_6$]·C$_6$H$_5$CN. The [ReCl$_6$]$^{2-}$ species lie on the (0,1/2,0) inversion centre, oriented with a triangular face of the Cl octahedron parallel to the BEDT-TTF layer, and are compressed slightly in the direction parallel to the BEDT-TTF long axes. The benzonitrile is disordered about the (1/2,0,0) inversion centre, with 50% occupation of each of the inversion-related positions. Unlike κ-(BEDT-TTF)$_4$[PtCl$_6$]·C$_6$H$_5$CN salt, where the six-fold carbon ring is centred about the inversion centre, the inversion-related atoms of the benzonitrile molecule are not superposed. Attempts at anisotropic refinement of the benzonitrile molecule gave very high correlation owing to the close atomic proximity of the two inversion-related orientations. Isotropic modelling led to a successful distinction between the two, giving the expected geometry and sensible temperature factors.

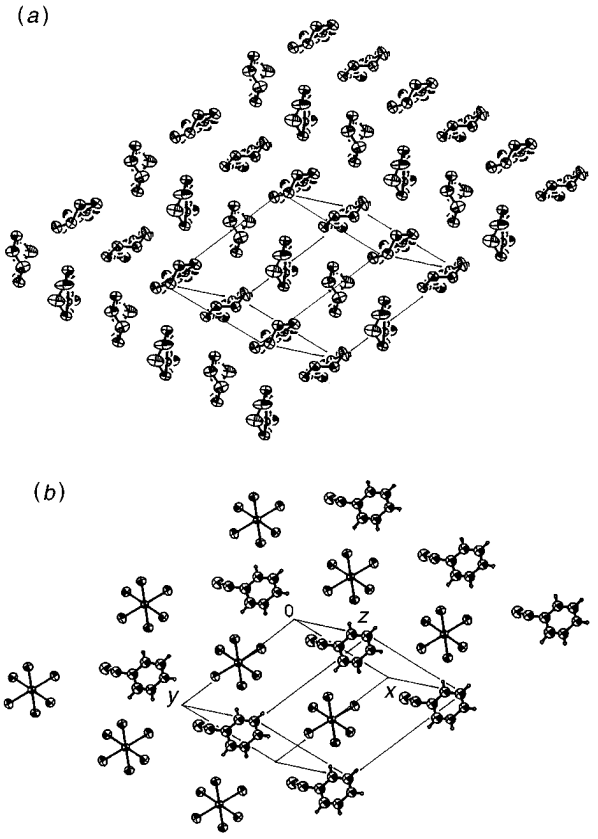

Fig. 3 Projection of the cation (*a*) and anion (*b*) layers of α-(BEDT-TTF)$_4$[ReCl$_6$]·C$_6$H$_5$CN down the BEDT-TTF axis (for clarity only one orientation of the disordered C$_6$H$_5$CN molecule is shown)

Band structure. There are eight independent nearest-neighbour interactions between the two independent BEDT-TTF molecules, as defined in Fig. 4. The calculated transfer integrals closely reflect the variations in intermolecular S—S distances, being moderate between the stacks, and only very small in the stacking direction (Table 3). The bond-over-bond stacking interactions F and H are significantly stronger than the translated interactions E and G. The estimated energy differences ΔE_{HOMO} between the HOMOs of molecules of type A and B are large with respect to the calculated transfer integrals, indicating the extent of localisation between the independent stacks, as also evidenced by the charge estimated through bond length analysis. A value for ΔE_{HOMO} of 200 meV was chosen for the purpose of the band-structure calculation.

The calculated band structure (shown with the Fermi surface in Fig. 5) predicts a semi-metallic state, with pairs of electron pockets located at $\pm b^*/2$ and hole pockets at $\pm a^*/2$. Measurement of electrical conductivity, magnetic susceptibility and infrared reflectivity, however, show the material to be

Table 3 Calculated transfer integrals, *t*′, HOMO energy differences and intermolecular S—S distances of α-(BEDT-TTF)$_4$[ReCl$_6$]·C$_6$H$_5$CN

			intermolecular S—S distances ⩽4.0 Å/Å		
interaction[a]	*t*′	ΔE_{HOMO}/eV	inner–inner[b]	inner–outer[b]	outer–outer[b]
A	140	270	3.73, 3.80, 3.85	3.40, 3.67	3.46, 3.58
B	97	120	3.83, 3.86, 3.87, 3.94	3.57, 3.91	3.56, 3.70
C	68	300	3.82, 3.86, 3.93	3.71	3.53
D	64	140	3.73, 3.82, 3.95	3.51, 3.53	3.45, 3.52
E	6	0	3.78	—	—
F	32	0	3.86	—	—
G	9	0	3.69	—	—
H	28	0	—	—	—

[a]The interactions A–H are defined in Fig. 4. [b]Inner and outer denote S atoms of the TTF and bis(ethylenedithio)moieties respectively.

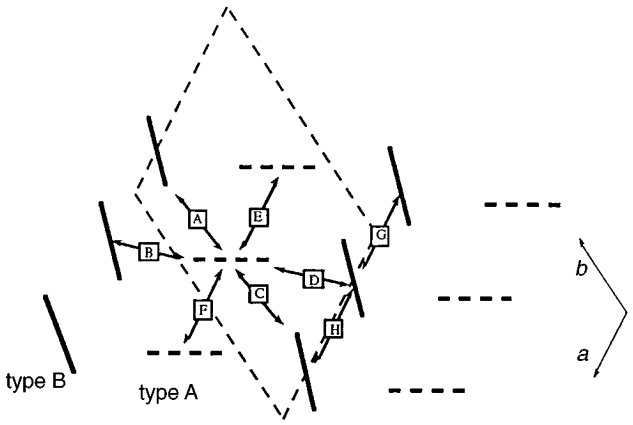

Fig. 4 Definition of the eight independent intermolecular BEDT-TTF interactions (A–H) in α-(BEDT-TTF)$_4$[ReCl$_6$]·C$_6$H$_5$CN

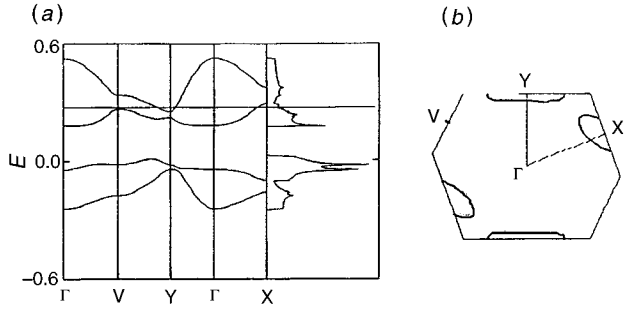

Fig. 5 Calculated band structure (*a*) and Fermi surface (*b*) of α-(BEDT-TTF)$_4$[ReCl$_6$]·C$_6$H$_5$CN

semiconducting. This discrepancy arises from the inadequacy of the extended Hückel model in taking account of electron correlation leading to localisation. However, important features that can be extracted include the high value of ΔE_{HOMO}, and the small intrastack transfer integrals E, F, G and H, which alternate in magnitude along the (BEDT-TTF) stacks.

The large difference in ionicity observed and the high ΔE_{HOMO} value suggest that there is only a very small degree of orbital mixing between the neighbouring donor stacks. Hence, the band structure may be crudely approximated by isolated one-dimensional stacks of A^+ and B^0. Semiconducting properties may be explained either in terms of an alternating delocalised A^+ stack, or by an A^+ Hubbard band (if the intrastack transfer integrals are sufficiently small to favour localisation).

Crystal and band structures of (BEDT-TTF)$_2$[IrCl$_6$]

Despite employing the same temperature and similar electrolyte concentrations as in the synthesis of α-(BEDT-TTF)$_4$[ReCl$_6$]·C$_6$H$_5$CN, a different phase is formed by [IrCl$_6$]$^{2-}$. (BEDT-TTF)$_2$[IrCl$_6$] crystallises in the $P\bar{1}$ space group, with an asymmetric unit containing (BEDT-TTF)$^+$ and half the [IrCl$_6$]$^{2-}$ units. There is no solvent of crystallisation. Atomic coordinates, bond lengths and angles, and thermal parameters have been deposited at the Cambridge Crystallographic Data Centre (see earlier; ref. no. 1145/22). Selected intramolecular bond lengths and angles are listed in Table 4, and the shortest intermolecular S—S distances may be found adjacent to the calculated intermolecular transfer integrals in Table 5.

The structure of (BEDT-TTF)$_2$[IrCl$_6$] represents a new packing motif among BEDT-TTF salts, and is unusual in containing no discrete layers of cations and anions. Face-to-face BEDT-TTF dimers oriented in the ring-over-bond conformation lie diagonally across the unit cell (see Fig. 6). A three-dimensional interacting network of such dimers is formed by the end-to-end interactions with neighbouring cells. The [IrCl$_6$]$^{2-}$ sits on the inversion centres at the corners of the cell, and is compressed slightly in the direction parallel with the BEDT-TTF axis. The Ir—Cl bond lengths are approximately equal.

Table 4 Selected intramolecular bond lengths (Å) and angles (degrees) of (BEDT-TTF)$_2$[IrCl$_6$]

Ir(1)—Cl(1)	2.320(2)	S(1)—C(1)	1.717(5)
Ir(1)—Cl(2)	2.328(2)	S(1)—C(3)	1.746(7)
Ir(1)—Cl(3)	2.322(2)	S(2)—C(1)	1.719(6)
		S(2)—C(4)	1.743(6)
Cl(1)—Ir(1)—Cl(2)	90.6(1)	S(3)—C(2)	1.720(6)
Cl(1)—Ir(1)—Cl(3)	88.3(1)	S(3)—C(5)	1.740(7)
Cl(2)—Ir(1)—Cl(3)	89.0(1)	S(4)—C(2)	1.713(5)
		S(4)—C(6)	1.748(7)
		C(1)—C(2)	1.400(9)
		C(3)—C(4)	1.344(6)
		C(5)—C(6)	1.358(7)

The shortest intermolecular S—S contacts occur within the dimer, which is distorted to minimise the distances between the inner S atoms (Table 5). The two independent inner S—S distances of 3.37 and 3.49 Å are extremely short, being much less than the sum of the van der Waals radii (3.7 Å). In contrast, there are few short S—S contacts between neighbouring dimers.

There is a potential ambiguity in the charge assignment in this salt, since the hexachloroiridate anion may exist in either the dinegative or the trinegative state.[7] Analysis of the intramolecular BEDT-TTF bond lengths by the δ-method[6] gives a charge of 1.05(1)+, suggesting that the correct formulation is (BEDT-TTF$^+$)$_2$[Ir^{IV}Cl$_6$] rather than (BEDT-TTF$^{1.5+}$)$_2$[Ir^{III}Cl$_6$]. The rather long BEDT-TTF central C—C bond (1.400 Å) suggests a further concentration of positive charge owing to the strong face-to-face dimer interaction. Accordingly, the neighbouring bond lengths are compatible with a lower charge. The average Ir—Cl bond length of 2.323 Å is very similar to the Pt—Cl length of 2.318 Å. A further uncommon aspect is that both BEDT-TTF ethylene groups are well ordered in the boat conformation [Fig. 6(*b*)] because of the steric interaction with the anion.

Intermolecular overlap. (BEDT-TTF)$_2$[IrCl$_6$] is one of the few examples of BEDT-TTF charge-transfer salts where significant intermolecular overlap occurs in all three directions (Table 5). However, despite the large number of neighbours, only four significant independent interactions occur. The very strong bond-over-bond intra-dimer interaction vastly exceeds all those to neighbouring cells, which are smaller owing to the end-to-end orientation and the longer S—S contacts. Hence localisation of charge in the form of (BEDT-TTF)$_2^{2+}$ is expected to dominate the electrical properties.

Electrical conductivity

Both the ReCl$_6$ and IrCl$_6$ salts are semiconducting, the former with a temperature-dependent activated behaviour [Fig. 7(*a*)]. Room-temperature conductivities of the ReCl$_6$ salt are relatively high for a semiconductor [σ_{RT}(along plate)≈3 S cm^{-1} and σ_{RT}(through plate)≈0.03 S cm^{-1}]. There is evidence for a subtle transition at 250 K [see inset to Fig. 7(*a*)], above which there is a constant activation energy, E_a, of 0.07 eV. Below the transition the activation energy is larger, varying between 0.1 and 0.15 eV. The sharp increase at 250 K may be due to localisation towards BEDT-TTF$_A^{1+}$ and BEDT-TTF$_B^0$, representing a transition from two-dimensional to one-dimensional behaviour. The gradual decrease in E_a below the 250 K transition is reminiscent of many one-dimensional conducting materials,[8] and is consistent with the one-dimensional electron hopping model. The upturn below *ca.* 110 K, however, represents a deviation from this behaviour. The strong crystallo-

Table 5 Transfer integrals, t, and intermolecular S—S distances of (BEDT-TTF)$_2$[IrCl$_6$]

interaction			intermolecular S—S distances ⩽4.0 Å/Å		
cell	molecule	t/meV	inner–inner[a]	inner–outer[a]	outer–outer[a]
0,0,0	A*	672	3.37, 3.49	—	3.92
1,0,0	A*	140	—	3.74, 3.84, 3.94, 4.03	—
0,1,0	A	19	—	4.05	3.88
	A*	0	—	3.66	3.37
0,−1,0	A	19	—	4.05	3.88
0,0,−1	A*	39	—	3.66	3.60
1,0,1	A	0	—	—	3.52

[a]Inner and outer denote S atoms of the TTF and bis(ethylenedithio) moieties respectively.

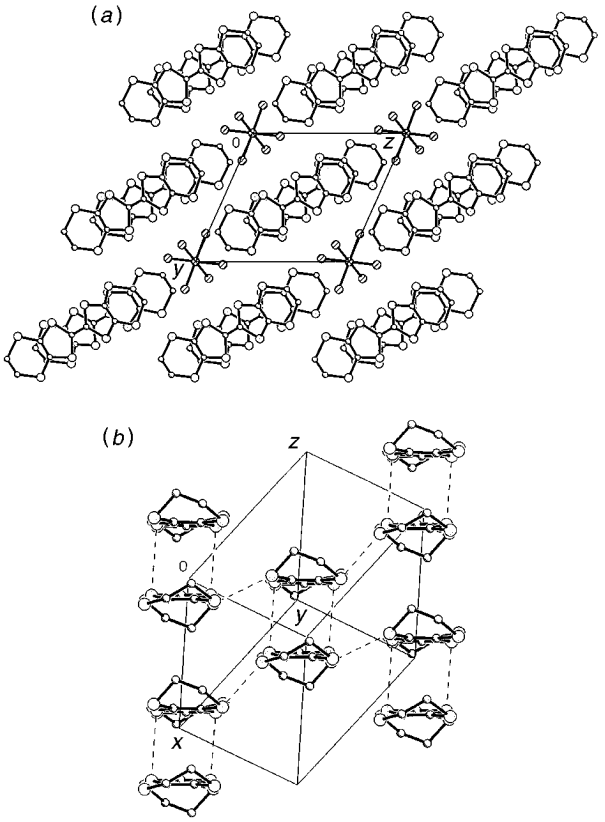

Fig. 6 Projection of the crystal structure of (BEDT-TTF)$_2$[IrCl$_6$] (*a*) down the *a* axis; (*b*) down the BEDT-TTF axis (the anion is omitted for clarity)

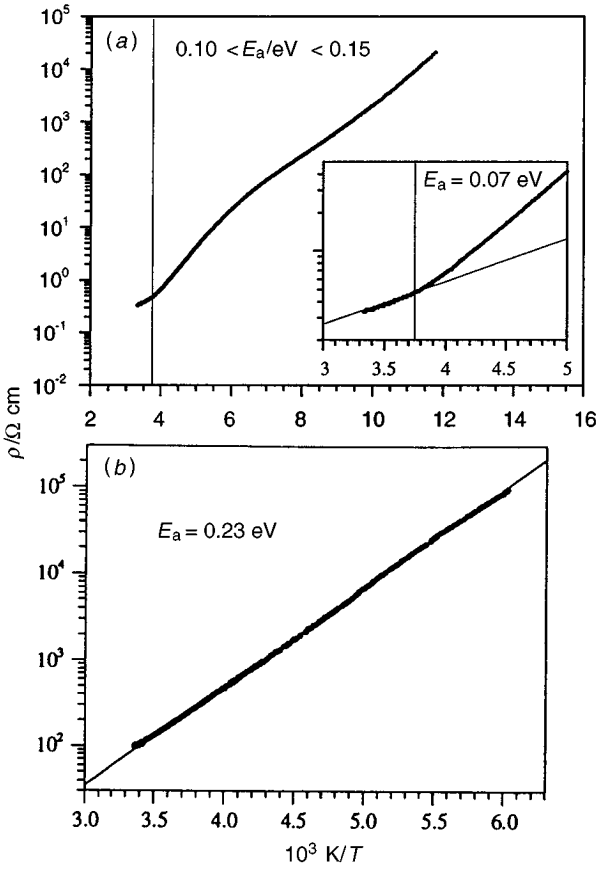

Fig. 7 Electrical transport of (*a*) α-(BEDT-TTF)$_4$[ReCl$_6$]·C$_6$H$_5$CN (along plate measurement), (*b*) (BEDT-TTF)$_2$[IrCl$_6$]

graphic evidence of ionicity, and the temperature-dependence of the activation energy, favours the Mott–Hubbard over the delocalised band picture. The IrCl$_6$ salt has a temperature-independent activation energy, $E_a = 0.23$ eV, from 180 to 300 K and a room-temperature conductivity, $\sigma_{RT} \approx 0.01$ S cm^{-1} [Fig. 7(*b*)].

Magnetic properties

α-(BEDT-TTF)$_4$[ReCl$_6$]·C$_6$H$_5$CN. The low-temperature magnetic properties of α-(BEDT-TTF)$_4$[ReCl$_6$]·C$_6$H$_5$CN are dominated by the Curie–Weiss behaviour of the anion [Fig. 8(*a*)], while at higher temperature a further Curie-like component due to the BEDT-TTF is superimposed. Based on the crystal structure and the transfer integral calculation, the susceptibility was modelled as the sum of Curie–Weiss and alternating antiferromagnetic chain contributions at high temperature.[9] For the case of a linear chain, the Hamiltonian for Heisenberg exchange interaction is

$$H = -2J \sum_{i=1}^{n} \boldsymbol{S}_{i-1}\boldsymbol{S}_i$$

For the more general case of an antiferromagnetic chain with exchange constants J_1 and J_2 alternating along the chain, the Hamiltonian becomes

$$H = -2J_1 \sum_{i=1}^{n/2} (\boldsymbol{S}_{2i-1}\boldsymbol{S}_{2i} + \alpha \boldsymbol{S}_{2i}\boldsymbol{S}_{2i+1})$$

where $\alpha = J_2/J_1$.

The temperature dependence of the susceptibility of a uniform Heisenberg antiferromagnetic linear chain was given by Bonner and Fisher,[10] and, for the high-temperature region, was fitted to the expression

$$\chi_m = \frac{Ng^2\mu_B^2}{kT} \cdot \frac{A + Bx + Cx^2}{1 + D + Ex^2 + Fx^3}$$

where $x = |J|/kT$.

The values $A = 0.25$, $B = 0.14995$, $C = 0.30094$, $D = 1.9862$, $E = 0.68854$, $F = 6.0626$ fit with a maximum disagreement of only 0.5% for $T > J/2k$. The susceptibility of the alternating Heisenberg antiferromagnetic chain obeys this equation,[11] with coefficients defined as polynomial expansions in α.[12] The

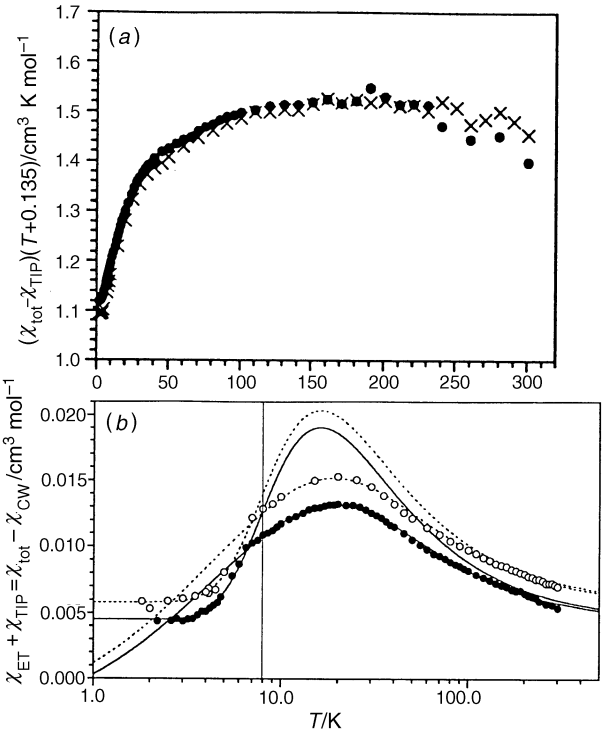

Fig. 8 (*a*) Temperature dependence of the effective Curie constant of α-(BEDT-TTF)$_4$[ReCl$_6$]·C$_6$H$_5$CN (x, 250 G; ●, 1000 G). (*b*) Fitting of the residual susceptibility of α-(BEDT-TTF)$_4$[ReCl$_6$]·C$_6$H$_5$CN to the alternating AF chain model ($T>8$ K, $J_1=16$ K, $J_2=13$–5 K, $\alpha=0.84$) and the Bleaney–Bowers model ($T<8$ K, $J<13$ K). (○, 250 G; ●, 1000 G.)

coefficients are valid for $T>J_1/2k$. At 6.5 K there is a definite break in the susceptibility, so below 6 K it was fitted to the sum of Curie–Weiss and dimer components. For the latter, the susceptibility is given by

$$\chi_m=\frac{2Ng^2\mu_B{}^2/kT}{3+\exp(-2J/kT)}$$

Iterative refinement gave, for the anion, $C=1.10(1)$ emu K mol^{-1} and $\theta=-0.135(5)$ K, and, for the BEDT-TTF chains, $\alpha=0.84$, $J_1=16$ K, $J_2=13$ K and $n=62\%$. The residual susceptibility after subtracting the Curie–Weiss component due to the anion is shown in Fig. 8(*b*) with fittings to the alternating chain model ($T>8$ K) and dimer model ($T<6$ K).

Finally, there is evidence for a subtle transition at 250 K, above which the cation susceptibility falls below the expected behaviour [Fig. 8(*a*)]. This feature matches the small sharp increase in the activation energy of electrical conduction.

(BEDT-TTF)$_2$[IrCl$_6$]. The magnetic properties of (BEDT-TTF)$_2$[IrCl$_6$] are dominated by an $S=1/2$ Curie–Weiss component, confirming the (BEDT-TTF$^+$)$_2$[IrCl$_6$]$^{2-}$ charge assignment. The total susceptibility was modelled at high temperature by the sum of the Curie–Weiss and Bleaney–Bowers equations, giving $C=0.234$ emu K mol^{-1}, $\theta=-0.37$ K for the anion and $J=670$ K. For (BEDT-TTF$^+$)$_2$ the exchange constant is exceptionally high for a BEDT-TTF salt, and results from the very short face-to-face interaction within the dimer pair. The 50-fold increase of the inter-dimer exchange constant of the IrCl$_6$ salt over the ReCl$_6$ one arises from the smaller interplanar separation in the former (*ca.* 3.35 compared to *ca.* 3.8 Å).

Infrared reflectance

Polarised spectra of α-(BEDT-TTF)$_4$[ReCl$_6$]·C$_6$H$_5$CN suggest moderate anisotropy in the room-temperature band structure. A large broadened feature centred at 1370 cm^{-1} arises from coupling of the free electron with the donor C=C stretching mode, as has been seen in many other salts.[13] Further weak sharp vibrational peaks occur at 780, 885, 1018, 1267 and 1410 cm^{-1}. The unpolarised spectrum of (BEDT-TTF)$_2$[IrCl$_6$] has a reflectivity lower than 20% in the range 700–4300 cm^{-1}, characteristic of a semiconductor. The most prominent vibrational peak at 1410 cm^{-1} arises from the ν(C=C) mode of BEDT-TTF. Further weak sharp peaks occur at 705, 805, 879, 993, 1024, 1175, 1236, 1279 and 1343 cm^{-1}.

Conclusions

Two new crystalline BEDT-TTF charge-transfer salts, with octahedral transition-metal anions, α-(BEDT-TTF)$_4$[ReCl$_6$]·C$_6$H$_5$CN and (BEDT-TTF)$_2$[IrCl$_6$], have been synthesised and structurally characterised. With these anions no salts crystallised in the form κ-(BEDT-TTF)$_4$[MCl$_6$]·C$_6$H$_5$CN, the only previously reported BEDT-TTF phase with hexachlorometallate anions.[1] That three different phases form from benzonitrile solution with anions of similar size and charge is evidence for the subtle energetics of crystal growth in this series of compounds.

A general structure–property relationship has emerged for α-phase BEDT-TTF salts such that those with angles between neighbouring stacks of *ca.* 50° undergo a metal–insulator transition at intermediate temperature, whilst those with an angle of *ca.* 80° remain metallic to low temperature or may become superconducting.[14] Therefore α-(BEDT-TTF)$_4$[ReCl$_6$]·C$_6$H$_5$CN represents an unusual deviation from expected behaviour, being a semiconductor no doubt because of its low symmetry and the presence of dinegative anions. The intramolecular bond lengths indicate that a high degree of ionicity exists within the BEDT-TTF layers of both the α-ReCl$_6$ and κ-PtCl$_6$ phases, which clearly match the varying charge distribution within the anion layers. We propose that the electrostatic interaction between layers influences the HOMO energies of the molecules, thereby moderating the degree of orbital mixing. In the extreme case of the energy difference between the HOMO dominating over the intermolecular transfer integrals the band structure approximates to separate lattices of independent BEDT-TTF. In α-(BEDT-TTF)$_4$[ReCl$_6$]·C$_6$H$_5$CN the band structure corresponds to the simple case of alternate one-dimensional stacks of (BEDT-TTF)$^+$. The semiconducting behaviour is therefore attributed to the strongly varying charge distribution in the anion layer owing to the presence of the neutral solvent molecules, which significantly influences the electronic energies of the BEDT-TTF cation layers.

In (BEDT-TTF)$_2$[IrCl$_6$] we have found a new packing arrangement of BEDT-TTF, with face-to-face dimers forming a three-dimensional interacting network. The BEDT-TTF bond lengths strongly favour a monopositive charge, a conclusion substantiated by the absence of any observable reaction between neutral BEDT-TTF and [IrCl$_6$]$^{2-}$ in solution. The magnetic susceptibility also favours the charge assignment (BEDT-TTF)$_2{}^{2+}$[IrCl$_6$]$^{2-}$ over (BEDT-TTF)$_2{}^{3+}$[IrCl$_6$]$^{3-}$. The very strong face-to-face intra-dimer interaction governs the electronic and magnetic properties of this salt, producing spin-paired (BEDT-TTF$^+$)$_2$.

The relatively high charge-to-size ratio of the [MCl$_6$]$^{2-}$ is an important factor in their crystallisation with BEDT-TTF. Whilst the inclusion of the large benzonitrile solvent molecule facilitates the formation of charge-ordered stacks of BEDT-TTF in the ReCl$_6$ salt, a phase containing BEDT-TTF$^+$ is obtained when the dinegative anion crystallises alone, as in the IrCl$_6$ salt.

The contribution of the BEDT-TTF to the magnetic susceptibility is difficult to separate from the Curie–Weiss contribution due to the paramagnetic anions, although it is clear

that the cations form antiferromagnetic chains. In α-(BEDT-TTF)$_4$[$ReCl_6$]·C_6H_5CN bond length considerations suggest that the orbital components of the conduction and valence bands derive primarily from the A^+ molecule. Hence, magnetically the salt may be considered as containing a one-dimensional alternating chain of A^+ with $\alpha = 0.84$ and $J_1 = 16$ K. In (BEDT-TTF)$_2$[$IrCl_6$] the one-dimensional stacks along the *a* direction are dimerised strongly, and the small increase in susceptibility at high temperature fits a dimer model with $J \approx 670$ K. The results therefore reveal a large increase in magnetic exchange interaction on shortening the face-to-face separation between the BEDT-TTF units. To clarify the extent of any interaction between the organic and inorganic spin systems in these novel phases it will be necessary to synthesise isostructural salts with diamagnetic $[MCl_6]^{2-}$.

We acknowledge support from EPSRC and the EU Human Capital and Mobility Programme. C.J.K. is the recipient of a Hackett Scholarship of the University of Western Australia. We are grateful to Dr. W. Hayes for access to the infrared spectrometer, and to Drs. P. Guionneau and L. Ducasse for assistance with the transfer integral and band-structure calculations.

References

1 A. A. Galimzyanov, A. A. Ignatev, N. D. Kushch, V. N. Laukhin, M. K. Makova, V. A. Merzhanov, L. P. Rozenberg, R. P. Shibaeva and E. B. Yagubskii, *Synth. Met*., 1989, **33**, 81.
2 V. E. Korotkov, V. N. Molchanov and R. P. Shibaeva, *Sov. Phys. Crystallogr*., 1993, **37**, 776.
3 M. Z. Aldoshina, L. S. Veretennikova, R. N. Lubovskaya and M. L. Khidekel, *Transition Met. Chem*., 1980, **5**, 63.
4 L. Ducasse, A. Abderrabba, J. Hoaran, M. Pesquier, B. Gallois and J. Gaultier, *J. Phys. C: Solid State Phys*., 1986, **19**, 3805; L. Ducasse and A. Fritsch, *Solid State Commun*., 1994, **91**, 201.
5 K. Bender, I. Hennig, D. Schweitzer, K. Dietz, H. Endres and H. J. Keller, *Mol. Cryst. Liq. Cryst*., 1984, **108**, 359.
6 P. Guionneau, C. J. Kepert, D. Chasseau, M. R. Truter and P. Day, *Synth. Met*., in press.
7 F. A. Cotton and G. Wilkinson, *Advanced Inorganic Chemistry*, Wiley, New York, 1988, 5th edn.
8 E. M. Conwell, in *Semiconductors and Semimetals: Highly Conducting Quasi-One-Dimensional Organic Crystals*, ed. E. M. Conwell, Academic Press, New York, 1988, vol. 27, pp. 1–27.
9 W. E. Hatfield, W. E. Estes, W. E. Marsh, M. W. Pickens, L. W. ter Haar and R. R. Weller, in *Linear Chain Compounds*, ed. J. S. Miller, Plenum Press, New York, 1983, vol. 3, p. 43.
10 J. C. Bonner and M. E. Fisher, *Phys. Rev. A*, 1964, **135**, 640.
11 J. C. Bonner and H. W. J. Blöte, *Phys. Rev. B*, 1982, **25**, 6959.
12 W. E. Hatfield, *J. Appl. Phys*., 1981, **52**, 1985.
13 F. L. Pratt, W. Hayes, M. Kurmoo and P. Day, *Synth. Met*., 1988, **27**, 439.
14 M. Kurmoo, P. Day, A. M. Stringer, J. A. K. Howard, L. Ducasse, F. L. Pratt, J. Singleton and W. Hayes, *J. Mater. Chem*., 1993, **3**, 1161.

Paper 6/05878G; *Received* 27*th August*, 1996